Emissions 2016

Simulation and Analysis of After-Treatment Systems (ATS) for Opposed-Piston 2 stroke Engine

Nishit Nagar, Arunandan Sharma, Fabien Redon
Achates Power, Inc.

Balaji Sukumar, Andy Walker
Johnson Matthey

Abstract

In order to meet the upcoming emissions regulations without incurring excessive cost, OEMs are now considering alternative engine architectures, including the opposed-piston engine. The opposed-piston engine has several inherent advantages over conventional engine architectures. Achates Power has optimized the basic opposed-piston (OP) architecture, introducing a patented combustion system and thermally optimized design. The engine out emissions at various operating modes of the opposed piston engine for the steady state (SET cycle) have been measured. Further, Johnson Matthey's SCRT® (an integration of CRT® – Continuously Regenerating Technology and SCR – Selective Catalytic Reduction technologies) system performance has been investigated for the engine exhaust conditions of the Achates engine. JM's high fidelity kinetic models have been used to simulate the entire aftertreatment system. The diesel oxidation catalyst (DOC), catalyzed soot filter (CSF) and selective catalytic reduction (SCR) models were based on 1D modeling framework and the dual layer selective ASC was based on 1D+1D modeling framework. The simulation results show the effect of design parameters (like PGM loading and space velocity) on system performance such as passive regeneration, overall NOx conversion and NH_3 slip. The simulation analysis shows US 2010 emission requirements on SET cycle can be met with current product aftertreatment technology.

Introduction

With the passage of Euro 6, and the recent U.S. introduction of new CO2 limits for heavy-duty trucks and buses, vehicle and engine manufacturers are facing a daunting challenge. Compliance with these regulations requires significant financial investments in new technologies, all designed to increase fuel efficiency while decreasing emissions. But, to remain competitive, manufacturers cannot pass along these costs to fleet owners.

One solution to this problem is the opposed-piston engine. This engine, which has been optimized by Achates Power, was once widely used in a variety of applications including aviation, maritime and military vehicles. After overcoming the architecture's historical challenges, the Achates Power opposed-piston engine now delivers a step-wise improvement in brake thermal efficiency over the most advanced conventional four-stroke engines. In addition, with the elimination of parts such as the cylinder head and valve train, it is also less complex and less costly to produce—making it even more appealing to manufacturers.

In order to demonstrate the benefits of OP technology, Achates Power has developed a medium duty 4.9L multi-cylinder with propriety combustion system and thermal load management strategy. The steady state results from this engine have been presented earlier [23]. Improvements to the performance of the engine have been made since then. This paper provides the current status of BSFC performance.

Opposed piston engine has differences in engine out flow, temperature and emissions concentration compared to conventional 4- stroke engine. In order to meet tailpipe emissions for US2010 regulation, it is critical to understand the aftertreatment system requirements. Using measured engine out conditions and Johnson Matthey's high fidelity kinetic model for DOC, CSF, SCR and ASC, a study has been performed to understand aftertreatment requirements and capability of the engine to meet tail pipe emission levels.

Fundamental OP engine advantages

Opposed-piston, two-stroke engines were conceived in the 1800s in Europe and subsequently developed in multiple countries for a wide variety of applications, including aircraft, ships, tanks, trucks and locomotives. They maintained their presence throughout the twentieth century. An excellent summary of the history of opposed-piston engines can be found in the SAE book, Opposed-Piston Engines: Evolution, Use, and Future Applications by M. Flint and J.P. Pirault [1]. Produced initially for their manufacturability and high power density, opposed-piston, two-stroke engines have demonstrated superior fuel efficiency compared to their four-stroke counterparts. This section examines the underlying reasons for the superior fuel efficiency and emissions. The OP2S diesel engine has the following efficiency advantages compared to a conventional, four-stroke diesel engine:

Reduced Heat Losses

The Achates Power opposed-piston engine, which includes two pistons facing each other in the same cylinder, offers the opportunity to combine the stroke of both pistons to increase the effective stroke-to-bore ratio of the cylinder. As a thought experiment, when a two cylinder conventional engine with 1.1 stroke-to-bore is re-architected as a single cylinder opposed piston engine with both pistons operating in the same bore, it results in an OP engine with 2.2 stroke-to-bore ratio. This can be accomplished while maintaining the engine and piston speed of the conventional 4 stroke engine. To achieve the same stroke-to-bore ratio with a conventional 4-stroke engine, the mean piston speed would double for the same engine speed. This would severely limit the engine speed range and, therefore, the power output. The increase in stroke-to-bore

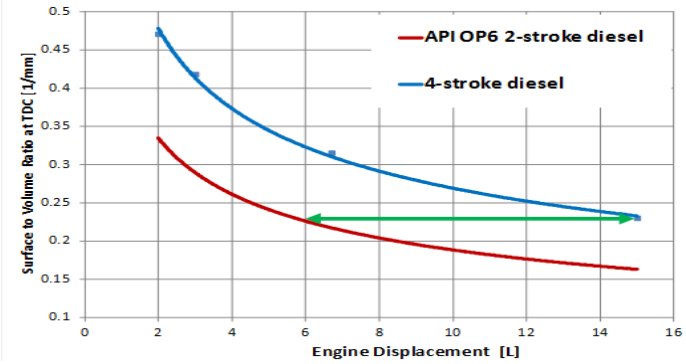

Figure 1: Surface-to-volume ratio versus engine displacement for an OP2S and conventional engine

ratio has a direct mathematical relationship to the area-to-volume ratio of the combustion space. Figure 1 shows the comparison a conventional 4 stroke engine to an opposed-piston engine with the same piston and crank dimensions. In this example, the reduction in the surface area to volume ratio is a very significant 36%. A 6 liter opposed piston engine has equivalent area-to-volume ratio as 15 liter conventional engine. The lower surface area directly leads to a reduction in heat transfer. An additional benefit of the reduced heat losses in the opposed-piston engine, especially for commercial vehicles, is the reduction in fan power and radiator size, further contributing to vehicle level fuel savings.

Leaner Combustion

When configuring an opposed-piston, two-stroke engine of the same displacement as a four-stroke engine –for example, converting a six-cylinder, conventional engine into a three-cylinder, opposed-piston engine – the power that each cylinder has to deliver is the same. The opposed-piston engine fires each of the three cylinders in each revolution while the four-stroke engine fires each of its six cylinders in one out of two revolutions.

Ideal Engine Efficiency

$$\eta_{ideal} = 1 - \frac{1}{r_c^{\gamma-1}}$$

r_c = compression ratio

γ = ratio of specific heats

Therefore, the amount of fuel injected for each combustion event is similar, but the cylinder volume is more than 50% greater for the Achates Power opposed-piston engine. So for the same boost conditions, the opposed-piston engine will

achieve leaner combustion, which increases the ratio of specific heat. Increasing the ratio of specific heat increases the work extraction per unit of volume expansion during the expansion stroke.

Faster and Earlier Combustion at the Same Pressure Rise Rate

The larger combustion volume for the given amount of energy released also enables shorter combustion duration while preserving the same maximum pressure rise rate. The faster combustion improves thermal efficiency by reaching a condition closer to constant volume combustion. The lower heat losses as described above lead to a 50% burn location

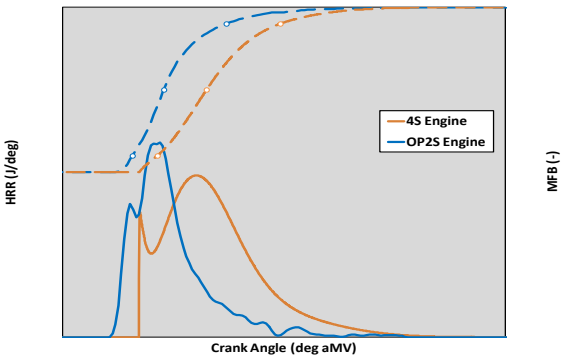

Figure 2: Heat release rate comparison between a four stroke and OP2S engine

closer to the minimum volume. Figure 2 illustrates how the heat release rate compares between a four-stroke engine and the Achates Power opposed-piston engine. The ideal combustion should occur at the minimum volume and be instantaneous. The opposed-piston engine is much closer to this ideal condition at the same pressure rise rate.

The aforementioned fundamental OP2S thermal efficiency advantages [2] are further amplified by:

- Lower heat loss due to higher wall temperature of the two piston crowns compared to a cylinder head (reduced temperature delta).
- Reduced pumping work due to uniflow scavenging with the OP2S architecture resulting in higher effective flow area than a comparable four-stroke or a single-piston two-stroke uniflow or loop-scavenged engine [5].
- Decoupling of pumping process from the piston motion because of the two-stroke architecture allows alignment of the engine operation with a maximum compressor efficiency line [6].

Efficiency and Emissions Enablers

Combustion System

Achates Power has developed a proprietary combustion system [3] composed of two identical pistons coming together to form an elongated ellipsoidal combustion volume where the injectors are located at the end of the long axis [4] (Figure 3).

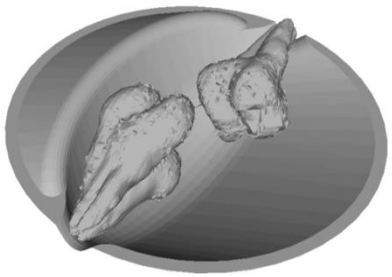

Figure 3: Schematic of the combustion system with plumes coming out of two side-mounted injectors

This combustion system allows the following -

- High turbulence, mixing and air utilization with both swirl and tumble charge motion with the high turbulent kinetic energy available at the time of auto ignition
- Ellipsoidal combustion chamber resulting in air entrainment into the spray plumes from two sides
- Inter-digitated, mid-cylinder penetration of fuel plumes enabling larger λ=1 iso-surfaces
- Excellent control at lower fuel flow rates because of two small injectors instead of a single higher flow rate
- Multiple injection events and optimization flexibility with strategies such as injector staggering and rate-shaping [7]

The result is no direct fuel spray impingement on the piston walls and minimal flame-wall interaction during combustion. This improves performance and emissions [8] with fewer hot spots on the piston surfaces that further reduce heat losses [7].

\Air System

To provide a sufficient amount of air for combustion, two-stroke engines need to maintain an appropriate pressure difference between the intake and exhaust ports. For applications that require the engine to change speed and load in a transient manner, such as automotive applications, external means of air pumping are required. Among the various possible configurations of the air system with turbocharger and supercharger combinations, the layout as described in Figure 4 is the preferred configuration [9].

Advantages of such an air system are summarized as follows:

- The compressor provides high pressure before the supercharger, which is further boosted by the supercharger. This means that low supercharger pressure ratios are sufficient for high intake manifold density, reducing pumping work.

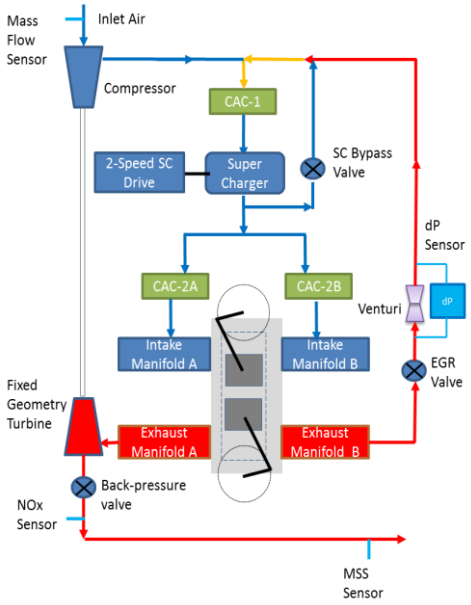

Figure 4: Schematic of air system layout for Achates Power's OP2S engine

- The maximum required compressor pressure ratio is lower compared to regular turbo-only air systems of four-stroke engines.
- The use of a supercharger recirculation valve allows greater control of the flow through the engine, thus providing flexibility for precise control of boost, scavenging ratio, and trapped residuals to minimize pumping work and NOx formation across the engine map
- Lowering the flow through the engine by decreasing the pressure difference across the engine reduces the pumping penalty at low load points. This, together with having no dedicated intake and exhaust stroke for moving mass from and to the cylinder improves BSFC.
- The supercharger and recirculation valve improves transient response [10].
- Accurate control of the engine pressure differential provides very good cold start and catalyst light off capabilities [11]. Low-speed torque is increased by selecting the appropriate gear ratios on the supercharger [8].

– Drive EGR with a supercharger reduces the required pumping work [8].
– Cool air and EGR together reduces fouling of the coolers [8][12].

Multi-Cylinder OP Research Engine Platform

A48-316 multi-cylinder platform that was used to generate the results presented in this paper. This multi-cylinder research engine was designed to meet the performance levels shown in the Table **1**.

Table 1: Achates Power's A48-316 OP2S engine specification

Displacement	4.9 L
Arrangement, number of cylinders.	Inline 3
Bore	98.4 mm
Displaced Stroke	215.9 mm
Stroke-to-Bore Ratio	2.2
Compression Ratio	15.4:1
Nominal Power (kW @ rpm)	205 @ 2200
Max. Torque (Nm @ rpm)	1100 Nm @ 1200-1600
Emission level	US 2010/ Euro 6

This engine was conceived as a research test platform and it utilizes oversized components and systems to provide significant level of flexibility required for exploring the capabilities of the engine. As a result, the size of the engine and the friction that has to be overcome is higher than expected from an optimized production engine. Figure 5 depicts the engine on the test bed during the testing.

Engine Architecture

Figure 5 provides an overview of the air-path for 3-cylinder Achates OP2S diesel engine. Upstream of the engine, a compressor driven by fixed-geometry turbo is used to draw in fresh air. To aid the airflow across the engine, there is a supercharger driven by a 2-speed drive that allows it to run at two different supercharger-to-engine speed ratios. For this engine, two drive ratios that were used are 3.2 and 4.6. A supercharger recirculation valve is used to control the airflow across the engine. Supercharger also creates positive differential pressure across the EGR loop to drive flow from exhaust manifold to compressor outlet. A venturi in the EGR loop with a delta-pressure sensor mounted across it is used to measure the EGR mass-flow. EGR valve is used to control the EGR flow to the engine. Downstream of the engine, a back-pressure valve is used to maintain the back-pressure of a clean after-treatment system.

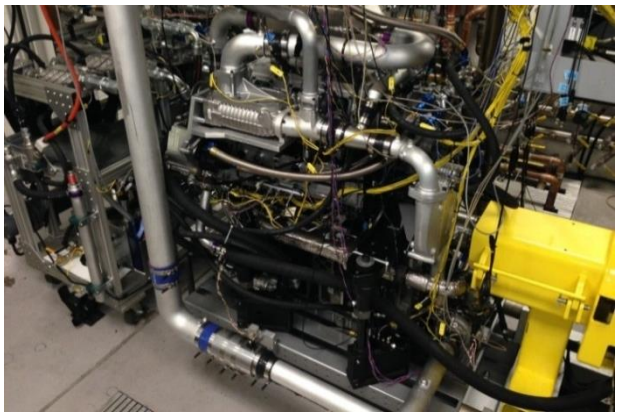

Figure 5: A48-316 engine setup in test cell

Dynamometer System and Test Cell instrumentation

The dynamometer system consists of a SAJ SE-400 eddy current absorber unit with a capacity of 400kW and 2000Nm. The inertia offered by the dyno is 0.82kg-m^2. The engine is coupled to the absorber with a Cardan shaft of 10,000Nm capacity. The speed-control loop of the dynamometer is executed at a frequency of 200Hz. Since this is an absorbing dynamometer, it is not possible to execute the motoring portion of the any test cycle. During such instances of the cycle, 10% of the brake-torque relative to the engine speed is commanded. Unlike a transient dynamometer, this dynamometer does not support closed-loop torque control to meet torque set-points. Torque profile is forwarded to ECU over CAN and ECU software has a torque-to-fuel map that generates fuel command to meet desired torque. Torque is measured by a Honeywell torque sensor (TMS9250) which is capable of measuring from 0 Nm to 4000Nm with an accuracy of +/- 4Nm. The torque flange is mounted in the driveline between the engine and the dyno-absorber. Zero-offset correction is performed before the test to account for any drift in the sensor measurement. Soot was measured using real-time AVL483 micro soot sensor. The soot number reported by AVL483 corresponds to elemental carbon content of total particulate mass. Engine out NOx was measured using both FTIR (for steady state operation) and real time Continental NOx sensor (for transient operation). Other gaseous emissions (HC and CO) were also measured using MKS FTIR. The NOx numbers reported in the results section are as measured by the emission bench and have been corrected for humidity as per EPA CFR 40 part 1065.

Steady state engine measurement

As mentioned earlier, A48-316 engine was created as a research platform to quickly iterate through different designs. In creating such a platform, some compromises were made versus how a production engine would be designed. Some examples of the experimental aspects of the engine include:

- Higher overall engine mass for robustness
- Larger package size for modular/swappable components
- Off-the-self air system components – supercharger, turbocharger and coolers that are not tuned for the engine
- Higher friction due to oversized off-the-shelf connecting rod big end and main bearings; aftermarket oil and coolant pumps; remote mounted gearbox with redundant bearings causing over constraint; dual dry sump scavenging pumps and air-oil separators
- Modular external gearbox connecting the exhaust and intake crank
- Modular front end accessory drive

In spite of the negative impact of the friction, steady-state fuel consumption measurement for the test-engine while meeting engine out emissions compatible with US EPA 2010 levels is compelling enough to showcase the potential benefits of OP2S engine. The steady state results for 13 modes of the SET cycle are shown in Table **2**

Table 2: 13 mode steady state performance of A48-316 engine

		Idle	A25	A50	A75	A100	B25	B50	B75	B100	C25	C50	C75	C100
Speed	RPM	799.9	1400	1400	1400	1400	1800	1800	1800	1800	2200	2200	2200	2200
Torque	Nm	7.8	290.8	550.7	824.5	1091.0	267.5	527.6	781.8	1018.6	228.5	444.9	665.3	882.2
Brake Power	bhp	0.9	57.2	108.3	162.1	214.6	67.6	133.4	197.7	257.6	70.6	137.5	205.6	272.7
BSFC	g/kWh	-	210.3	198.5	196.3	197.0	217.5	194.9	192.0	196.6	234.5	205.9	198.3	198.8
BSNOx	g/bhp-hr	-	1.6	2.9	3.1	3.0	1.9	2.9	2.9	3.6	1.5	1.9	1.7	1.5
BSSoot	g/bhp-hr	-	0.03	0.01	0.01	0.02	0.03	0.01	0.01	0.02	0.03	0.02	0.01	0.03
BSCO	g/bhp-hr	-	0.4	0.2	0.8	2.3	0.5	0.2	0.6	1.8	0.5	0.2	0.2	1.0
BSHC	g/bhp-hr	-	0.1	0.1	0.1	0.1	0.1	0.1	0.1	0.1	0.1	0.1	0.1	0.1
Indicated Thermal Efficiency	%	33.2	49.9	50.7	49.4	48.4	51.8	52.0	50.6	49.2	51.5	52.7	52.5	51.5
Brake Thermal Efficiency	%	-	39.9	42.2	42.7	42.5	38.5	43.0	43.6	42.6	35.7	40.7	42.3	42.2
Friction Loss	%	25.3	8.7	5.9	4.4	3.5	10.8	7.1	5.2	4.8	12.3	8.6	7.3	6.5
Pumping Loss	%	3.0	1.3	2.5	2.2	2.3	2.5	1.9	1.8	1.8	3.4	3.4	3.0	2.8
Air/Fuel Ratio	-	101.8	30.7	32.1	27.6	25.6	34.7	29.3	24.5	22.8	32.5	30.1	25.5	22.5
EGR rate	%	35.5	30.5	30.4	28.8	27.1	30.1	26.3	26.1	21.6	31.8	30.8	31.6	29.3
Turbine Out Temp	deg C	150.5	260.4	256.4	291.5	312.5	235.8	276.0	320.6	356.5	250.5	253.3	287.0	327.9
Turbine Out Pressure	bar A	1.0	1.03	1.06	1.10	1.14	1.05	1.08	1.11	1.16	1.06	1.09	1.13	1.17

The cycle average BSFC for this data set is 200 g/kWh with best point BSFC of 192 g/kWh. The cycle average results are shown in Table **3**.

Table 3: SET cycle average results for A48-316 engine

13 Mode SET Cycle Results		
Cycle Average Results		
BSFC	200	g/kWh
BSNOx	2.58	g/bhp-hr
BSSoot	0.016	g/bhp-hr
BSCO	0.98	g/bhp-hr
BSHC	0.07	g/bhp-hr

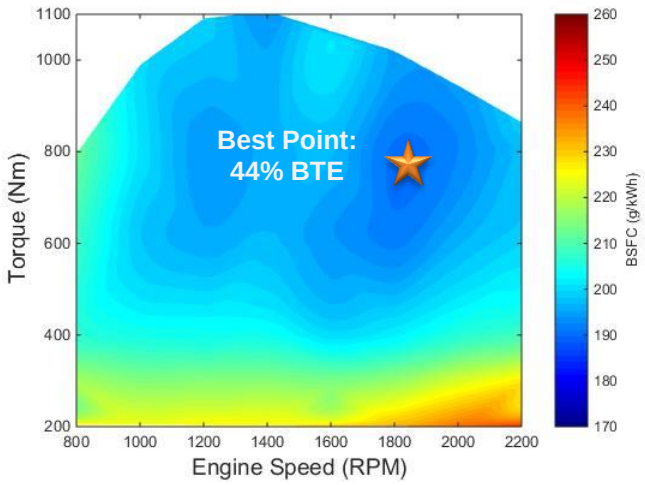

Figure 6: Measured BSFC map of A48-316 engine

Figure **6**, 7a and 7b show the fuel, soot and NOx map respectively for the entire torque curve of the engine. The engine has a flat fuel map as can be seen in Fig 7. For the 12 operating modes at A, B and C speed the difference between the best point and cycle average is only 8 g/kWh. A grounds-up design for 4.9L engine that has been optimized friction and air handling system is expected to deliver 182 g/kWh cycle average BSFC with best point efficiency of 176 g/kWh [23].

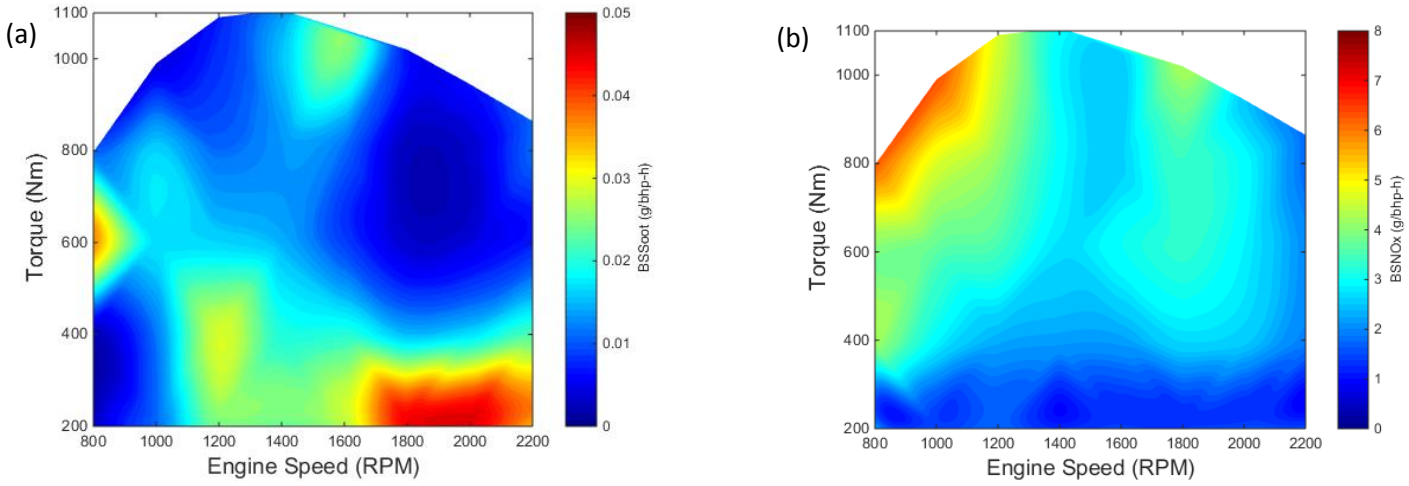

Figure 7: (a) Measured BSSoot in g/bhp-hr for A48-316 engine, (b) Measured BSNOx in g/bhp-hr for A48-316 engine

After-treatment system Introduction

Engine out emission results from SET cycle show that the Achates opposed piston engine (OP2S) has very low CO and HC emissions. With better BSFC, the engine out temperature is low which may challenge the periodic soot removal from the after-treatment filter system. However, the engine out NOx is relatively high (~3.5g/kwh), which would assist the passive regeneration of a DPF leading to balance point. In addition, to meet EPA10 regulation limits, the NOx conversion across the ATS should be high. In this section, we investigate Johnson Matthey's patented SCRT® (Figure 9: an integration of CRT® – Continuously Regenerating Technology and SCR – Selective Catalytic Reduction technologies) system – the 4-way emission control technology suitable for this engine.

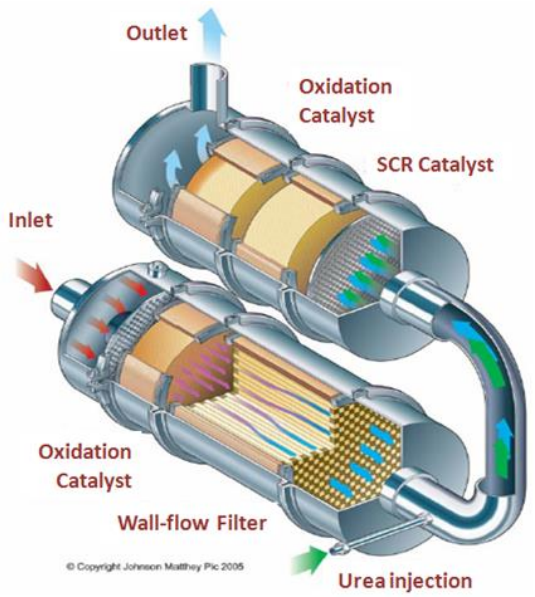

Figure 9: Johnson Matthey's SCRT® System

Diesel engines are usually fitted with four after-treatment system components to abate CO, HC, NOx, PM and NH_3 emissions. The first component is the Diesel Oxidation Catalyst (DOC) with platinum group metals - PGM (Pt or Pd) to oxidize HC and CO in the exhaust. In addition, the DOC plays an important role in both attaining passive regeneration for the DPF and high NOx reduction in the downstream catalysts by oxidizing NO to NO_2. The second component is the Catalyzed Soot Filter (CSF) to remove particulate matter from the exhaust stream. The filter is coated with PGM to improve NO oxidation and in turn improve passive soot oxidation. PGM in the filter also helps in combusting further HC and CO that slips out of the DOC during active regeneration or high space velocity conditions. Filter substrate properties are to be chosen carefully for good ash capacity and Particle Number (PN) regulations. The third component is a selective reduction catalyst (SCR) which is proven to be very effective in reducing NOx. Urea is used as a reductant which hydrolyzes to produce NH_3. When the inlet NO_2/NOx is high (50%), fast SCR reaction takes place instantaneously at temperatures >200°C leading to significantly high NOx conversion. Although stoichiometric amount of NH_3 is required to reduce NOx, due to the NH_3 storage functionality in the catalyst and due to the dynamic nature of the feed conditions, urea is usually over injected into the SCR catalyst to increase NOx conversion. This results in NH_3 slip from the SCR catalyst. Hence a fourth component – Ammonia Slip Catalyst (ASC) is used to oxidize the excess NH_3 selectively to N_2. The sizing of these four components, the formulation type and PGM loading in the DOC and the CSF are to be optimized for a given application to satisfy the emissions regulation limits.

Fully developed and validated high fidelity models for DOC, coated Filter (CSF), SCR (Cu- based) and ASC (Cu- based) formulations have been used in this study. DOC and SCR models are developed using a 1D modeling framework. A 1D single channel pair model was used to represent the CSF. That is, the CSF modeling framework consists of two parts: i) describing axial flow in the channels, and temperature effects in the filter; and ii) describing soot accumulation and removal, NO oxidation within the filter wall, and NO_2 diffusion from the wall to the soot cake. A 1D+1D model was

developed for the selective Cu- based ammonia slip catalyst. Complex kinetics are developed for each formulation to capture the catalyst behavior at both spatial and temporal coordinates and at varied feed conditions the catalyst will be subjected in a real world scenario.

Component Models:

A number of monolith catalyst modeling studies for both flow through and filter substrates are available extensively in the literature. The state-of-the-art modeling activities at Johnson Matthey on multiple catalyst formulations and after-treatment system configuration have been previously published for gasoline, light and heavy duty diesel applications. More details about the modeling framework used in this study can be found elsewhere (DOC[14], CSF[15], SCR[16] and ASC[17]). It is worthwhile to mention that a number of assumptions were made in the monolith model; the major assumptions are listed below:

1) uniform flow distribution at the monolith entrance.

2) negligible radial concentration and temperature profiles.

3) transport of mass and energy in the gas by convection.

4) transport of energy in the solid by conduction.

5) description of the transfer of mass and energy between the gas and the solid uses coefficients derived from a correlation available in the literature [18].

6) no diffusion resistance is present in the catalyst washcoat.

After-treatment System Analysis: Steady state engine test

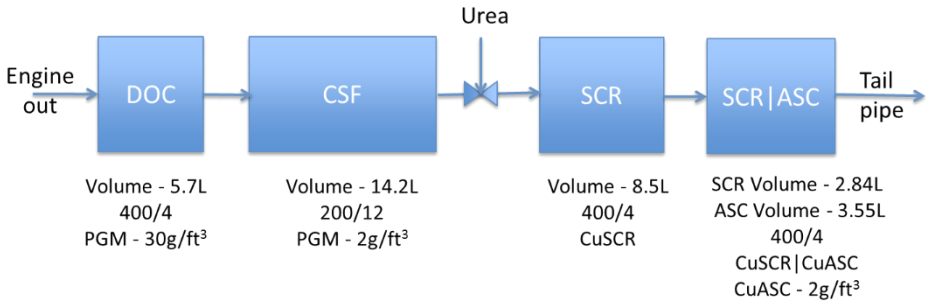

Figure 10: After-treatment system architecture used in this study

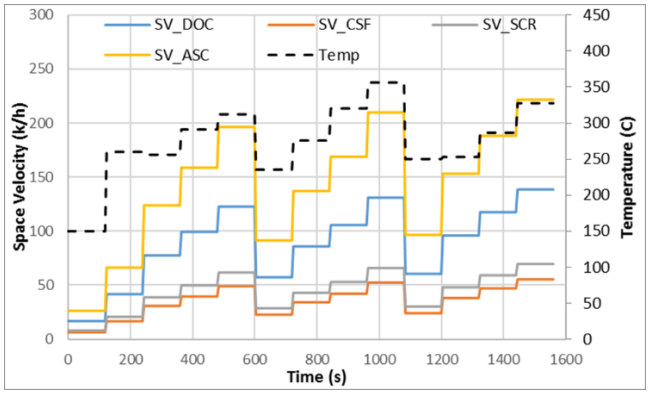

Figure 11: Temperature and SV of each component in the ATS during the 13 mode SET cycle

The ATS investigated in this study along with details on the catalyst technology, catalyst volume, PGM loading and CPSI/wall thickness are shown in Figure 10. The volume of each component is initially chosen based on the exhaust flow rate such that the maximum space velocity (SV) for DOC, CSF, SCR and ASC is ~140, 55, 70 and 220 k/h respectively.

13 mode steady state engine test (SET cycle) results were used and the ATS was simulated using the models developed for specific formulations. Figure 11 shows the temperature and the SV in each component for the 13 modes. Each mode is simulated for 120s followed by a ramp up to the next mode condition in 5s. It can be seen that the temperature ranges between ~236°C to 356°C and the temperature during idling is at 150°C.

The simulation results are discussed in this section for each component from engine out to tailpipe. The engine out emissions are initially used to simulate the DOC performance. Based on an extensive study [19] on the effect of Pt:Pd ratio in DOCs, hydrocarbon oxidation activity generally increases with the increase in Pt fraction in Pt-Pd catalysts. For propylene and toluene oxidation, there is an optimal Pt:Pd ratio that would give highest oxidation performance, while for decane oxidation the activity increases monotonically as a function of Pt content. Unlike hydrocarbon oxidation, CO oxidation performance decreases with an increase in Pt:Pd ratio. NO oxidation activity is directly related to the fraction of Pt in the catalyst. In order to capture the effect of DOC performance on the overall passive regeneration of the system, two DOCs of different characteristics were considered – 1. Low Pt:Pd (2:1) ratio aged at 780°C/10h and 2. High Pt: Pd (5:1) ratio aged at 700°C/100h. Both models represent severely aged conditions – to represent end of useful life characteristics. The two DOC models were chosen so that the NO oxidation is different (low and high) to investigate the effect of NO_2/NOx on the soot balance point and the overall NOx reduction.

While the DOC removes HC and CO from the exhaust stream, it also oxidizes the NO to NO_2, which can be utilized to oxidize the PM in the filter. When the exhaust temperature and NOx/PM ratio are high enough [20], the soot accumulation in the filter can be reduced without needing any servicing or high temperature active regeneration operations (>500°C). The reaction between soot and NO_2 enables passive regeneration to occur leading to continued operation at acceptable back pressure limits. However, in some applications the exhaust conditions can be more challenging with low temperature and low NOx/PM ratio. Under such situations, a catalyzed filter is used. By coating a PGM based catalyst on the filter helps in continued passive regeneration. In a bare filter, NO_2 oxidizes soot to form NO which cannot be further utilized for soot oxidation. In the presence of an oxidizing catalyst in the filter, the NO formed will in turn be oxidized to NO_2 which will again be used for soot oxidation, due to the effective back diffusion of NO_2 from catalyst or filter wall into the soot layer. Hence in a CSF, each NO molecule can potentially be reused multiple times before it leaves the filter. In this study, a 2g/ft^3 Pt only CSF is used.

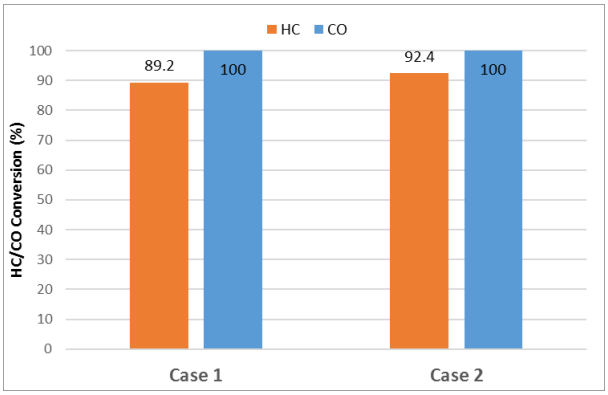

Figure 12: HC and CO conversion efficiency over DOC+CSF in the 13 mode SET cycle

As indicated in Table 2, the total hydrocarbon (THC) emissions at all modes is around 0.1g/kwh and CO emissions is ~0.3 to 3.1g/kwh. This translates to <45ppm THC and ~46 to 500ppm of CO. The HC speciation from engine out can vary based on engine and the operating conditions. For this study, it is assumed to be 74% Decane, 4% Toluene and 22% Propylene in the simulations. The details on HC and CO light off characteristics of different DOC types can be obtained elsewhere ([19], [21]). Figure 12 shows the percentage conversion of HC and CO after DOC+CSF for the two DOC types considered in this study. Case 1 represents 2:1 Pt:Pd DOC and Case 2 represents 5:1 Pt:Pd DOC. As the temperature in SET cycle is always higher than the light off temperature of CO, 100% CO combustion can be obtained. THC combustion using a 5:1 DOC provides a slightly better conversion efficiency (~92.4% at CSF out) compared to a 2:1 DOC (89.2% at CSF out). The tailpipe emissions for both HC and CO as predicted by the simulations are provided in Table 5. The results clearly show that HC and CO regulation limits can be easily attained in both cases as the engine out emissions are relatively low and the temperatures in all the modes are within the favorable range.

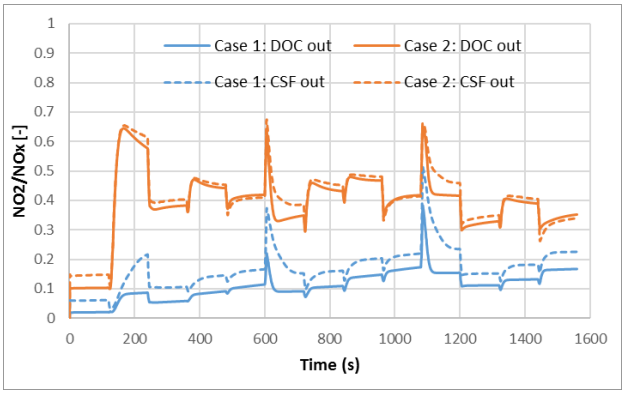

Figure 13: NO oxidation over DOC and CSF in the 13 mode SET cycle

Figure 13 differentiates the performance of two DOCs on NO_2/NOx. The engine out NO_2/NOx was assumed to be 10%. It can be seen that with case 2 DOC, outlet NO_2/NOx is around 40%. With case 1 DOC, it is mostly less than 20%. The simulation was carried out with 0g/l initial soot loading and hence there was no NO_2 consumption in the filter. As there is PGM in the filter, there is a slight increase in NO_2/NOx from DOC out to CSF out. This changes the soot accumulation mechanism over a prolonged time in the filter (Figure 14). The 13 mode SET cycle was simulated for 100 cycles consecutively to predict how much soot is accumulated over time. Case 1 DOC with low NO_2/NOx does not reach balance point after 100 cycles (>4.3 g/l soot loading). On the other hand, Case 2 DOC with better NO_2/NOx at CSF inlet helps in passive regeneration. Balance point is reached at ~1.3g/l. If the CSF inlet NO_2/NOx is not sufficiently high, the PGM loading in CSF can be increased to increase the NO oxidation in the filter. In this study, the effect of upstream DOC on passive regeneration is of interest and hence the PGM loading in CSF is maintained constant. In order to compare the difference between a coated and an uncoated filter, additional simulation was carried out for case 1 (with low DOC out NO_2/NOx). With an uncoated filter, the overall soot loading after 100 cycles is higher than the 2g/ft^3 CSF. With high PGM loading in the CSF (say, 4 to 6g/ft^3) soot oxidation can be enhanced further. This shows that to attain better passive regeneration, both DOC and CSF formulations need to be chosen or optimized appropriately.

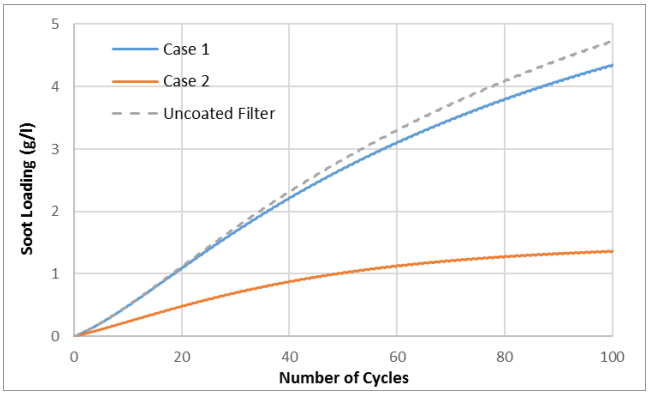

Figure 14: Soot loading over the CSF using case 1 and case 2 DOC, and DPF using case 1 DOC over 100 SET cycles

With HC, CO and PM removed by the DOC and CSF, the next step is to remove NOx. An SCR catalyst is now introduced along with urea injection. Urea hydrolyzes at high temperatures (>200°C) to produce NH_3 which is used by the SCR catalyst to reduce NO and NO_2 via the standard, fast and slow SCR reactions [16]. There are many SCR formulations (eg., Fe-, V- and Cu-based) that can be used for different applications, based on the requirements. For this study, as the engine out temperature is low, an SCR that can provide better performance at low temperatures, like Cu-SCR, is chosen. The cumulative NOx at SCR in and SCR out for ammonia to NOx ratio (ANR) of one is shown in Figure 15a. The simulation is initialized with zero NH_3 stored on the catalyst and the cycle is repeated four times such that the NH_3 stored in the catalyst bed reaches pseudo steady state. The results from the last cycle (5th cycle) are provided.

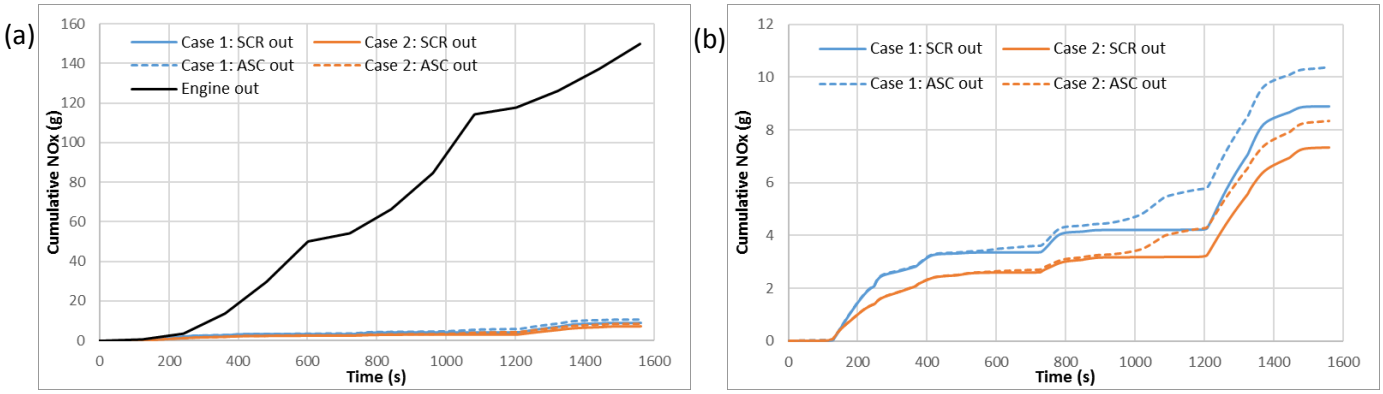

Figure 15: NOx conversion efficiency over the 13 modes SET cycle (last cycle from the five consecutive cycle simulation) a. NOx at SCR in, SCR and ASC out, b. Zoomed in plot of SCR and ASC out NOx emissions

The results show that more than 96% NOx conversion can be achieved. NH_3 slip from SCR during high temperature excursions is oxidized in the ASC. The ASC catalyst is a dual layer catalyst with DOC functionality in the bottom layer and Cu-SCR in the top layer. The selectivity of this catalyst to N_2 is high. However, there will be some NOx remake at high temperatures [17] which may affect the overall (tailpipe) NOx conversion efficiency. This is shown in Figure 15b. The tailpipe NOx emissions are provided in Table 5 which clearly shows that the NOx target limit can be easily reached with the proposed AT system.

Table 5: Engine out and tailpipe emissions for a 13 mode SET cycle

	Engine out (g/kwh)	**Tailpipe (g/kwh)**	
		Case 1	**Case 2**
CO	1.264	0	0
THC	0.102	0.011	0.008
NOx	3.47	0.138	0.120
N_2O	0	0.103	0.112

The mechanism behind SCR reaction is that the NH_3 in gas phase gets adsorbed onto the storage sites and the adsorbed NH_3 reacts with NO and/or NO_2. The NH_3 storage capacity of the catalyst decreases as the temperature increases. Hence a sudden increase in temperature will result in NH_3 desorption from the catalyst leading to NH_3 slip. This is seen in Figure 16a, which shows the NH_3 slip from SCR with case 1 and case 2 DOC. In the figure, as the temperature goes beyond 300°C, NH_3 from the catalyst is desorbed. With case 1 DOC, the NO_2/NOx at SCR inlet is low and hence mostly the standard SCR reaction takes place. However, with case 2 DOC, the NO_2/NOx at SCR inlet is appropriate for the fast reaction to take place. Hence, NOx conversion in SCR with case 2 DOC is higher than that with case 1 DOC. This results in more NH_3 consumption leading to less NH_3 slip. When the NO_2/NOx ratio is high, NH_4NO_3 formation happens on the SCR at low temperatures (~200°C) which decomposes at high temperatures to form N_2O. Therefore, case 2 SCR/ASC has slightly more N_2O formation (Figure 16b, Table 5) than case 1. Comparing SCR and ASC out N_2O emissions in Figure 16b, N_2O is formed over ASC when there is NH_3 slip from SCR around 300°C to 350°C. During this intermediate temperature range (300°C), the selectivity of the ASC is more towards N_2 (~81%) and to a lesser extent towards N_2O (~15%) and NOx (~4%).

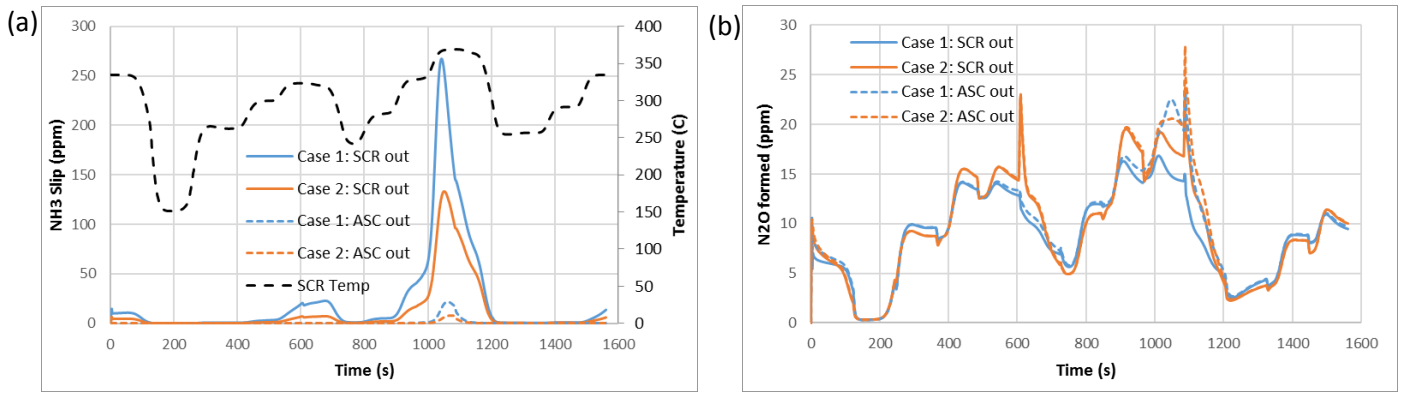

Figure 16: NH_3 slip and N_2O formed over SCR and ASC over the 13 modes SET cycle

Summary and Conclusion:

The A48-316 multi cylinder research engine developed by Achates Power has demonstrated cycle average BSFC of 200 g/kWh for the SET cycle with the best point efficiency of 192 g/kWh. This is despite the fact that the engine friction has not been optimized in order to preserve the flexibility of the engine to act as a research platform. A grounds-up OP2S engine with optimized friction and air handling components is expected to deliver 182 g/kWh on SET cycle. Based on the Achates power opposed piston engine out conditions from steady state cycle, it can be seen that the tailpipe HC, CO and PM targets can be reached relatively easily. The proposed after-treatment system with appropriate urea dosing is sufficient to maintain the NOx level below the EPA10 target along with low NH_3 slip and N_2O for SET cycle. All the models used in this study are based on catalyst formulations that are commercially available. The system performance can further be improved by using catalysts with better low temperature performance (eg. high active site density catalysts on high CPSI or HPS, new CuSCR technology, increased active site density and SCRF® technologies, thereby decreasing the ATS volume even further.

Acknowledgements:

The authors would like to thank Penelope Markatou at Johnson Matthey for valuable inputs on after-treatment systems simulation. The authors also would like to thank Achates Power Inc and Johnson Matthey Inc for permission to publish this paper.

Abbreviations:

OP2S – Opposed Piston 2 Stroke
PGM – Platinum Group Metal
DOC – Diesel Oxidation Catalyst
CSF – Catalyzed Soot Filter
DPF – Diesel Particulate Filter (uncoated)
SCR – Selective Catalytic Reduction
ASC – Ammonia Slip Catalyst
PN – Particulate Number
PM – Particulate Matter
SV – Space Velocity
SET – Supplemental Emissions Test (ESC – European Stationary Cycle)
SCRT® – Selective Continuously Regenerating Technology
THC – Total Hydrocarbon

References:

1. Flint, M. and Pirault, J.P., “Opposed Piston Engines: Evolution, Use, and Future Applications”, SAE International, Warrendale, PA ISBN 978-0-7680-1800-4, 2009.
2. Herold, R., Wahl, M., Regner, G., Lemke, J., and Foster, D., “Thermodynamic Benefits of Opposed-Piston Two-Stroke Engines,” SAE Technical Paper 2011-01-2216, 2011, doi: 10.4271/2011-01-2216.
3. Fuqua, K., Redon, F., Shen, H., Wahl, M., and Lenski, B., “Combustion Chamber Constructions for Opposed-Piston Engines”, U.S. Patent Application US20110271932.

4. Venugopal, R., Abani, N., MacKenzie, R., “Effects of Injection Pattern Design on Piston Thermal Management in an Opposed-Piston Two-Stroke Engine”, SAE International Technical Paper 2013-01-2423, 2013, doi:10.4271/2013-01-2423.
5. Regner, G., Naik, S., “Not All Two-Stroke Engines Are Created Equal”, Retrieved from http://www.achatespower.com/diesel-engine-blog/2013/09/27/not-all-two-stroke-engines-are-created-equal/, 2013.
6. Regner, G., “Turbocharger Efficiency: An Underappreciated OP2S Advantage”, Retrieved from http://www.achatespower.com/diesel-engine-blog/2013/01/23/turbocharger-efficiency/, 2013.
7. Venugopal, R., Abani, N., MacKenzie, R., “Effects of Injection Pattern Design on Piston Thermal Management in an Opposed-Piston Two-Stroke Engine”, SAE International Technical Paper 2013-01-2423, 2013, doi:10.4271/2013-01-2423.
8. Regner, G., Fromm, L., Johnson, D., Koszewnik, J., Dion, E., Redon, F., “Modernizing the Opposed-Piston, Two-Stroke Engine for Clean, Efficient Transportation”, SAE International Technical Paper 2013-26-0114, 2013, doi:10.4271/2013-26-0114.
9. Pohorelsky, L., Brynych, P., Macek, J., Vallaude, P., Ricaud, J., Obsernesser, P., Tribotté, P., “Air System Conception for a Downsized Two-Stroke Diesel Engine”, SAE International Technical Paper 2012-01-0831, 2012, doi:10.4271/2012-01-0831.
10. Ostrowski, G., Neely, G., Chadwell, C., Mehta, D., Wetzel, P., “Downspeeding and Supercharging a Diesel Passenger Car for Increased Fuel Economy”, SAE International Technical Paper 2012-01-0704, 2012.
11. 12.Kalebjian, C., Redon, F., and Wahl, M. “Low Emissions and Rapid Catalyst Light-Off Capability for Upcoming Emissions Regulations with an Opposed-Piston, Two-Stroke Diesel Engine”, Emissions 2012 Conference.
12. Teng, H. and Regner, G., “Characteristics of Soot Deposits in EGR Coolers”, SAE International Journal of Fuels and Lubricants, Vol. 2, No. 2, pp. 81-90, 2010. Also published as SAE Technical Paper 2009-01-2671, 2009, doi:10.4271/2012-01-0704.
13. Sharma. A, Redon F. , Multi-cylinder Opposed Piston Engine Results on Transient Test Cycle. To be presented at SAE 2016 world congress.
14. Ahmadinejad, M., Desai, M. R., Watling, T. C., York, A. P. E., “Simulation of Automotive Emission Control Systems”, Advances in Chemical Engineering, 33, 47-101, 2007
15. York, A., Ahmadinejad, M., Watling, T., Walker, A. et al., "Modeling of the Catalyzed Continuously Regenerating Diesel Particulate Filter (CCR-DPF) System: Model Development and Passive Regeneration Studies," SAE Technical Paper 2007-01-0043, 2007, doi:10.4271/2007-01-0043
16. Dai, J., Markatou, P., Johansson, A., Klink, W. et al., "Fe-Zeolite SCR Model Development, Validation and Application," SAE Technical Paper 2011-01-1304, 2011, doi:10.4271/2011-01-1304
17. Balaji, S., Dai, J., Johansson, A., Markatou, P. et al., "Modeling of Dual Layer Ammonia Slip Catalysts (ASC)," SAE Technical Paper 2012-01-1294, 2012, doi:10.4271/2012-01-1294
18. Ullah, U., Waldram, S. P., Bennett, C. J., Truex, T., “Monolithic reactors: mass transfer measurements under reacting conditions”, Chemical Engineering Science, 47, 2413-2418, 1992
19. Shakya, B., Sukumar, B., López-De Jesús, Y., and Markatou, P., "The Effect of Pt:Pd Ratio on Heavy-Duty Diesel Oxidation Catalyst Performance: An Experimental and Modeling Study," SAE Int. J. Engines 8(3):1271-1282, 2015, doi:10.4271/2015-01-1052
20. Allansson, R., Blakeman, P., Cooper, B., Hess, H. et al., "Optimising the Low Temperature Performance and Regeneration Efficiency of the Continuously Regenerating Diesel Particulate Filter (CR-DPF) System," SAE Technical Paper 2002-01-0428, 2002, doi:10.4271/2002-01-0428
21. Etheridge, J., Watling, T., Izzard, A., and Paterson, M., "The Effect of Pt:Pd Ratio on Light-Duty Diesel Oxidation Catalyst Performance: An Experimental and Modelling Study," SAE Int. J. Engines 8(3):1283-1299, 2015, doi:10.4271/2015-01-1053
22. Redon, F., Sharma, A., and Headley, J., “Multi-Cylinder Opposed Piston Transient and Exhaust Temperature Management Test Results,” SAE Techical Paper 2015-01-1251, doi:10.4271/2015-01-1251
23. Naik, S., Redon, F., Regner, G., and Koszewnik, J., "Opposed-Piston 2-Stroke Multi-Cylinder Engine Dynamometer Demonstration," SAE Technical Paper 2015-26-0038, 2015, doi:10.4271/2015-26-0038.